

## Probing light dark matter through cosmic-ray cooling in active galactic nuclei

Gonzalo Herrera<sup>1,2</sup> and Kohta Murase<sup>3,4,5</sup>

<sup>1</sup>*Physik-Department, Technische Universität München, James-Franck-Straße, 85748 Garching, Germany*

<sup>2</sup>*Max-Planck-Institut für Physik (Werner-Heisenberg-Institut),*

*Föhringer Ring 6, 80805 München, Germany*

<sup>3</sup>*Department of Physics; Department of Astronomy and Astrophysics;*

*Center for Multimessenger Astrophysics, Institute for Gravitation and the Cosmos,*

*The Pennsylvania State University, University Park, Pennsylvania 16802, USA*

<sup>4</sup>*School of Natural Sciences, Institute for Advanced Study, Princeton, New Jersey 08540, USA*

<sup>5</sup>*Center for Gravitational Physics and Quantum Information, Yukawa Institute for Theoretical Physics, Kyoto University, Kyoto, Kyoto 606-8502, Japan*

(Received 30 July 2023; revised 14 March 2024; accepted 21 June 2024; published 22 July 2024)

Recent observations of high-energy neutrinos from active galactic nuclei (AGN), NGC 1068 and TXS 0506 + 056, suggest that cosmic rays (CRs) are accelerated in the vicinity of the central supermassive black hole and high-energy protons and electrons can cool efficiently via interactions with ambient photons and gas. The dark matter density may be significantly enhanced near the black hole, and CRs could lose energies predominantly due to scatterings with the ambient dark matter particles. We propose CR cooling in AGN as a new probe of dark matter-proton and dark matter-electron scatterings. Under plausible astrophysical assumptions, our constraints on sub-GeV dark matter can be the strongest derived to date. Some of the parameter space favored by thermal light dark matter models might already be probed with current multimessenger observations of AGN.

DOI: 10.1103/PhysRevD.110.L011701

**Introduction.** The presence of dark matter (DM) in galaxies and clusters of galaxies is well established by astrophysical and cosmological observations [1]. However, its particle nature remains unknown [2]. A variety of experiments have aimed to detect DM particles via their scatterings off nuclei and/or electrons at Earth-based detectors, setting strong upper limits on the interaction strength of DM particles with masses in the GeV scale but leaving the sub-GeV region of the parameter space yet largely unconstrained [3–7]. Historically, DM fermions with sub-GeV masses were disfavored by the cosmological bound [8,9]. However, large parameter space still remains unexplored in more complicated but well-motivated scenarios [10–12].

Different approaches have been proposed to extend the sensitivity reach of direct detection experiments for sub-GeV DM. Some of these consider a boosted component of DM particles reaching Earth, via gravitational effects or via scatterings with protons, electrons, or neutrinos in different astrophysical environments (e.g., Refs. [13–29]).

Active galactic nuclei (AGN) are promising sources of high-energy protons and electrons. While the dominant acceleration mechanism of these cosmic rays (CRs) is still under debate, modeling of multimessenger data has placed important constraints on not only energetics of CR production, but also the emission region of the observed neutrinos that can be produced via either inelastic  $p p$  collisions or  $p \gamma$  interactions [30–32]. For example, observations of high-energy neutrinos and gamma rays from NGC 1068 [33,34] suggest that the neutrino production occurs in the vicinity of the supermassive black hole (SMBH) at  $R_{\text{em}} \lesssim (30\text{--}100)R_S$  (where  $R_S$  is the Schwarzschild radius), which is consistent with theoretical models [35–39], and the required proton luminosity is at least  $\sim 10\%$  of the intrinsic x-ray luminosity [40,41]. Another neutrino source candidate, TXS 0506 + 056 [42–46], is known to be a jet-loud AGN, the observed spectral energy distribution in photons is mostly explained by synchrotron and inverse-Compton emission from CR electrons [45,47–51], and the proton luminosity required by IceCube observations may even exceed the Eddington luminosity [47,48].

In this work, we propose CRs produced in AGN as a new, unique probe of DM-proton and DM-electron scatterings through their multimessenger observations. Given that emission regions of neutrinos and gamma rays are constrained to be near the SMBHs, CRs also need to traverse

Published by the American Physical Society under the terms of the [Creative Commons Attribution 4.0 International license](#). Further distribution of this work must maintain attribution to the author(s) and the published article's title, journal citation, and DOI. Funded by SCOAP<sup>3</sup>.

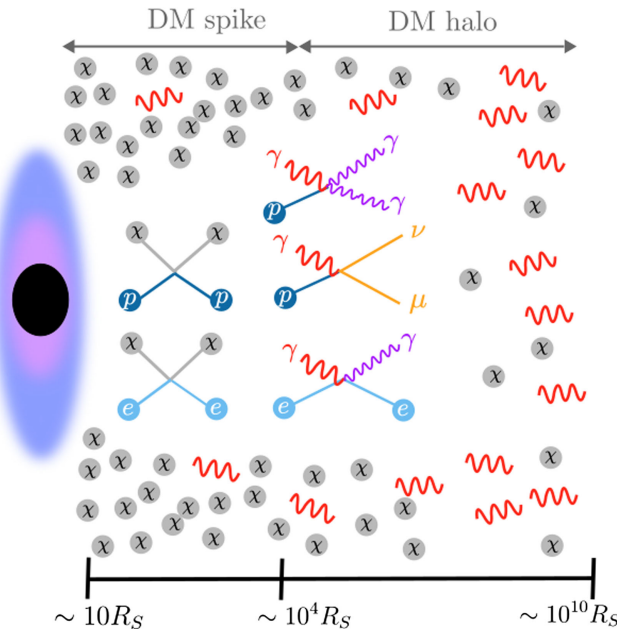


FIG. 1. Schematic picture of dark cooling of CRs due to elastic scatterings with DM particles in AGN. High-energy protons and electrons may traverse a high density of DM particles more efficiently than standard cooling processes involving neutrino and photon emission.

the DM spike around the central SMBH. If such additional cooling beyond the Standard Model (BSM) was too strong, CR energy losses are modified so that the required CR luminosity would be larger, and the neutrino and photon spectra could even be incompatible with the observations. Our work is different from previous studies on AGN probes of the DM scatterings with protons and electrons, which focused either on the boosted flux of DM particles from the source at Earth [22,52,53] or on the spectral distortions in the gamma-ray flux induced by CR scatterings off DM particles [54–59]. Instead, we focus on the impact of the DM-proton and DM-electron scatterings on the neutrino and photon fluxes or the CR power, considering for the first time the cooling of protons and electrons in the inner regions of the AGN, where a DM spike is likely to be formed (see Fig. 1).

TABLE I. Relevant parameters considered in this work for NGC 1068 and TXS 0506 + 056, for two different sets of assumptions dubbed (I) and (II). Here,  $R_{\text{em}}$  represents the distance of the emission region from the central SMBH in NGC 1068 (TXS 0506 + 056),  $M_{\text{BH}}$  shows the SMBH mass and its uncertainty,  $t_{\text{BH}}$  is the black hole age,  $r_0$  is the scale radius of the galaxy,  $\langle \sigma v \rangle / m_{\text{DM}}$  denotes the assumed values of the effective DM self-annihilation cross section, and  $\langle \rho_{\text{DM}} \rangle$  is the average density of DM particles within  $R_{\text{em}}$ .

	$R_{\text{em}}$	$M_{\text{BH}}$	$t_{\text{BH}}$	$r_0$	$\langle \sigma v \rangle / m_{\text{DM}}$	$\langle \rho_{\text{DM}} \rangle$
NGC 1068 (I)	$30R_S$	$(1\text{--}2) \times 10^7 M_\odot$	$10^{10}$ yr	10 kpc	0	$5 \times 10^{18} \text{ GeV/cm}^3$
NGC 1068 (II)	$30R_S$	$(1\text{--}2) \times 10^7 M_\odot$	$10^{10}$ yr	10 kpc	$10^{-31} \text{ cm}^3 \text{ s}^{-1}/\text{GeV}$	$4 \times 10^{13} \text{ GeV/cm}^3$
TXS 0506 + 056 (I)	$10^4 R_S$	$(3\text{--}10) \times 10^8 M_\odot$	$10^9$ yr	10 kpc	0	$8 \times 10^{12} \text{ GeV/cm}^3$
TXS 0506 + 056 (II)	$10^4 R_S$	$(3\text{--}10) \times 10^8 M_\odot$	$10^9$ yr	10 kpc	$10^{-28} \text{ cm}^3 \text{ s}^{-1}/\text{GeV}$	$4 \times 10^{11} \text{ GeV/cm}^3$

*DM distribution in AGN.* The adiabatic growth of black holes may form a spike of DM particles in their vicinity [60–63]. An initial DM profile of the form  $\rho(r) = \rho_0(r/r_0)^{-\gamma}$  evolves into

$$\rho_{\text{sp}}(r) = \rho_R g_\gamma(r) \left( \frac{R_{\text{sp}}}{r} \right)^{\gamma_{\text{sp}}}, \quad (1)$$

where  $R_{\text{sp}} = \alpha_\gamma r_0 (M_{\text{BH}}/(\rho_0 r_0^3))^{1/(3-\gamma)}$  is the size of the spike, with numerical values  $\alpha_\gamma$  provided in Ref. [62]. The cuspiness of the spike is given by  $\gamma_{\text{sp}} = \frac{9-2\gamma}{4-\gamma}$ . Furthermore,  $g_\gamma(r) \approx (1 - \frac{4R_s}{r})$ , while  $\rho_R$  is a normalization factor, chosen to match the density profile outside of the spike,  $\rho_R = \rho_0 (R_{\text{sp}}/r_0)^{-\gamma}$ . This density profile vanishes at  $4R_s$ , which is, however, a conservative approximation [64,65].

We consider that the initial DM distribution follows an Navarro-Frenk-White (NFW) profile [66,67], with  $\gamma = 1$ , resulting in a spike with  $\gamma_{\text{sp}} = 7/3$  and  $\alpha_\gamma = 0.122$ . The masses of the central SMBHs of the two AGN considered in this work are given in Table I. For the scale radius of both galaxies, we take  $r_0 = 10$  kpc. Finally, the normalization  $\rho_0$  is determined by the uncertainty on the SMBH mass [55,68], also provided in Table I. We have checked that these criteria yield masses of the DM halo compatible with those expected from universal relations between SMBH and galactic bulge masses [69,70]. We use Eq. (8) of Ref. [69].

If the DM particles self-annihilate, the maximal DM density in the inner regions of the spike is saturated to  $\rho_{\text{sat}} = m_{\text{DM}} / ((\langle \sigma v \rangle t_{\text{BH}})$ , where  $\langle \sigma v \rangle$  is the velocity averaged DM self-annihilation cross section and  $t_{\text{BH}}$  is the SMBH age. For TXS 0506 + 056 (NGC 1068), we take the value  $t_{\text{BH}} = 10^9$  ( $10^{10}$ ) yr [52,71]. Furthermore, the DM spike extends to a maximal radius  $R_{\text{sp}}$ , beyond which the DM distribution follows the initial NFW profile. The DM density profile therefore reads [62,68,72]

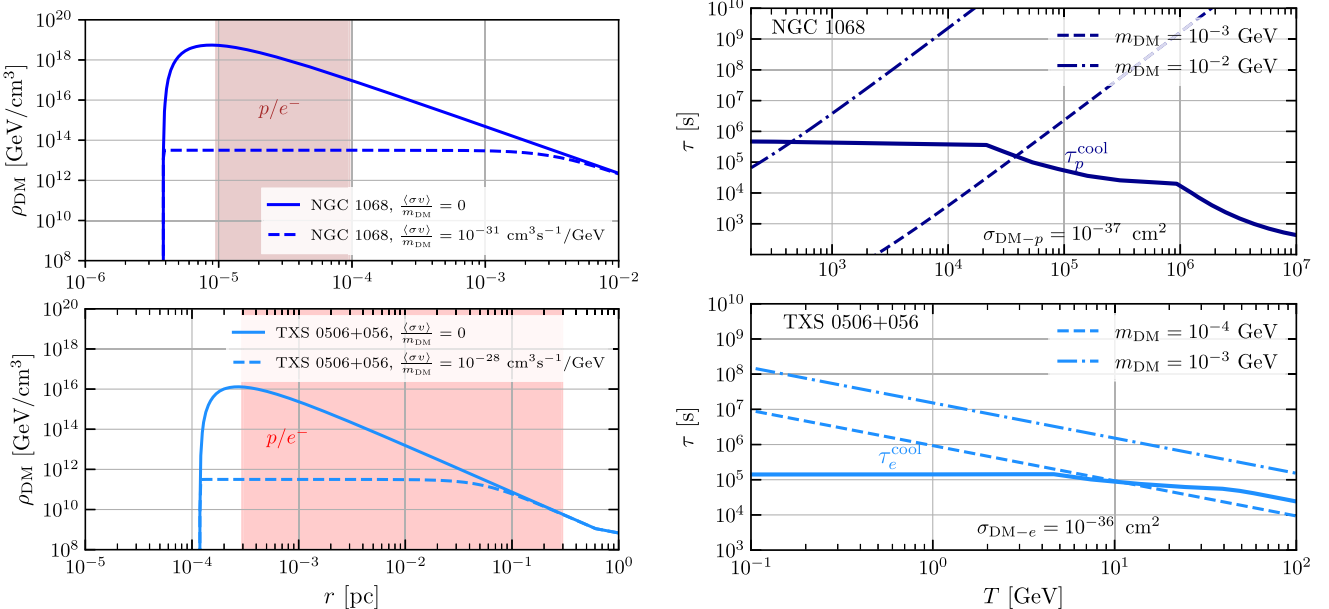


FIG. 2. Left panel: DM distribution around the SMBHs of TXS 0506 + 056 and NGC 1068, for different values of the DM self-annihilation cross section over its mass. The red (brown) shaded region indicates the region where the production of high-energy particles is expected to take place in TXS 0506 + 056 (NGC 1068). Right panel: In solid lines, we show the cooling timescales of protons (electrons) in NGC 1068 (TXS 0506 + 056). In dashed and dot-dashed lines, we show the timescales due to elastic DM-proton and DM-electron scatterings [40,45].

$$\rho(r) = \begin{cases} 0 & r \leq 4R_S, \\ \frac{\rho_{\text{sp}}(r)\rho_{\text{sat}}}{\rho_{\text{sp}}(r)+\rho_{\text{sat}}} & 4R_S \leq r \leq R_{\text{sp}}, \\ \rho_0 \left(\frac{r}{r_0}\right)^{-\gamma} \left(1 + \frac{r}{r_0}\right)^{-(3-\gamma)} & r \geq R_{\text{sp}}. \end{cases} \quad (2)$$

The DM profiles in TXS 0506 + 056 and NGC 1068 are shown in the left panel in Fig. 2 for two values of  $\langle \sigma v \rangle / m_{\text{DM}}$  allowed for sub-GeV DM [73–75]. We find that the DM density is extremely high in the region where high-energy particles are produced.

**BSM cooling of CRs in AGN.** Neutrinos and photons from AGN can be explained by emission from high-energy protons and electrons through purely SM mechanisms. Energy-loss mechanisms include scatterings with other SM particles in the plasma or synchrotron radiation as well as adiabatic losses. In addition, there are escape losses due to advection or diffusion via magnetic fields. The presence of DM coupling to protons and electrons in the vicinity of SMBHs would introduce additional scattering timescales, leading to the suppression of the observed neutrino and gamma-ray fluxes in certain energy ranges, if the BSM cooling timescales of CRs were shorter than the standard cooling timescales. For example, at  $m_{\text{DM}} \sim 10^{-3}$  GeV, the currently allowed maximum DM-proton cross section stems from CR-boosted DM at the Super-Kamiokande experiment [76], with a value of  $\sigma_{\text{DM}-p} \sim 10^{-35} \text{ cm}^2$ . As

discussed in the previous section, the average density of asymmetric DM particles in the coronal region of NGC 1068 is  $\langle \rho_{\text{DM}} \rangle \sim 5 \times 10^{18} \text{ GeV}/\text{cm}^3$ . Thus, if the corresponding cross section for CR protons is comparable to  $\sigma_{\text{DM}-p}$  (although this is not the case, in general), the BSM cooling timescale for the currently allowed values in the literature is  $\tau_{\text{DM}-p} \sim 1/(\langle n_{\text{DM}} \rangle \sigma_{\text{DM}-p} c) \sim 7 \times 10^3 \text{ s}$ , which is well below the proton cooling time inferred by observations of NGC 1068. This simple estimate clearly suggests that CRs in AGN can provide a powerful probe of these interactions.

More quantitatively, the BSM cooling timescale due to elastic DM scattering off CRs is given by [59]

$$\tau_{\text{DM}-i}^{\text{el}} = \left[ -\frac{1}{E} \left( \frac{dE}{dt} \right)_{\text{DM}-i} \right]^{-1}, \quad (3)$$

with

$$\left( \frac{dE}{dt} \right)_{\text{DM}-i} = -\frac{\langle \rho_{\text{DM}} \rangle}{m_{\text{DM}}} \int_0^{T_{\text{DM}}^{\max}} dT_{\text{DM}} T_{\text{DM}} \frac{d\sigma_{\text{DM-CR}i}}{dT_{\text{DM}}}, \quad (4)$$

where  $\langle \rho_{\text{DM}} \rangle$  is the average density of DM particles in the region of CR production. See Table I for the specific values that we use for NGC 1068 and TXS 0506 + 056. Also,  $d\sigma_{\text{DM-CR}i}/dT_{\text{DM}}$  is the differential elastic DM-proton or DM-electron cross section, and  $T_{\text{DM}}^{\max}$  is the maximal allowed value for  $T_{\text{DM}}$  in a collision with a particle  $i$  with kinetic energy  $T = E - m_i$ , which is

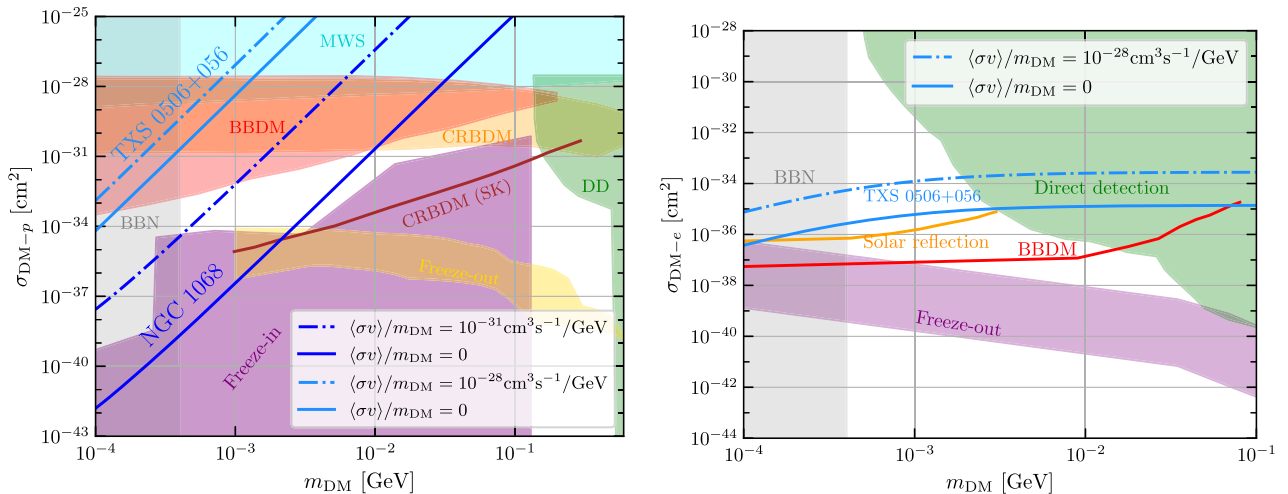


FIG. 3. Left panel: upper limits on the DM-proton cross section vs DM mass, derived from the requirement that the required proton luminosity is substantially larger due to scatterings off DM particles in NGC 1068 and TXS 0506 + 056. Complementary constraints from different searches are shown for comparison. We also show values of the DM-proton scattering cross section that can produce the observed DM relic abundance via freeze-in (purple) [80,81] and via freeze-out (gold) [82,83]. Right panel: analogous upper limits on the DM-electron cross section, for TXS 0506 + 056. We also display values of the DM-electron cross section vs DM mass compatible with thermal production of light DM [84]. This band shows the range of values compatible with thermal production in different models (scalar dark matter [85], asymmetric dark matter [73], strongly interacting massive particles [12,86], and elastically decoupling relics [87]). Note that we do not have constraints from NGC 1068, because the observed gamma rays may be purely hadronic [34].

$$T_{\text{DM}}^{\max} = \frac{2T^2 + 4m_i T}{m_{\text{DM}}} \left[ \left( 1 + \frac{m_i}{m_{\text{DM}}} \right)^2 + \frac{2T}{m_{\text{DM}}} \right]^{-1}. \quad (5)$$

We consider fermionic DM which elastically interacts with protons and electrons via a heavy scalar mediator. The differential cross section reads [77]

$$\frac{d\sigma_{\text{DM-CR}i}}{dT_{\text{DM}}} = \frac{\sigma_{\text{DM}-i}}{T_{\text{DM}}^{\max}} \frac{F_i^2(q^2)}{16\mu_{\text{DM}-i}^2 s} (q^2 + 4m_i^2)(q^2 + 4m_{\text{DM}}^2), \quad (6)$$

where  $\sigma_{\text{DM}-i}$  is the DM-proton or DM-electron cross section at the zero center-of-mass momentum,  $\mu_{\text{DM}-i}$  is the reduced mass,  $s$  is the square of center-of-mass energy, and  $q^2 = 2m_{\text{DM}}T_{\text{DM}}$  is the momentum transfer of the process. The quantity  $F_i$  is either the proton form factor [78] or equal to 1 for electrons.

In the right panel in Fig. 2, the solid lines represent the total standard energy-loss timescales as a function of energy for protons in NGC 1068 [40] and for electrons in TXS 0506 + 056 [79]. CR protons in NGC 1068 are almost depleted, and the dominant cooling mechanisms at increasing energies are inelastic  $p p$  interactions, Bethe-Heitler pair production, and  $p\gamma$  interactions [35]. CR protons do not cool efficiently in TXS 0506 + 056, and the fate is governed by a dynamical timescale of  $\sim 10^5$  s in the SMBH frame [79]. For electrons in TXS 0506 + 056, the dominant cooling mechanisms are inverse Compton scattering and synchrotron radiation. The breaks in the solid lines of the

plots reflect the energies at which the transition of dominant processes occurs.

For comparison, we also show BSM cooling timescales due to elastic DM scatterings with protons and electrons. The dot-dashed line corresponds to values of the DM mass and cross section that would induce a contribution smaller than the proton and electron energy losses due to the SM processes. On the other hand, the dashed line shows values of the parameters that would induce larger energy losses than in the SM at relevant energies. It is important to point out that inelastic DM-proton scatterings are expected to dominate over the elastic channel at energies  $E \gtrsim m_p^2/2m_{\text{DM}}$ . For simplicity, we restrict our analysis to the elastic channel.

For the purpose of constraining the interaction strength, we find for each  $m_{\text{DM}}$  the largest DM-proton (electron) cross section yielding a timescale equal or larger to the cooling timescales determined with models at relevant energies. In particular, we use

$$\tau_{\text{DM}-i}^{\text{el}} \geq C\tau_i^{\text{cool}}. \quad (7)$$

The coefficient  $C$  is a model-dependent factor, and we use  $C = 0.1$  in this work. In other words, we find the maximum DM-proton (electron) cross section that would have an  $\mathcal{O}(10)$  or less impact on the proton (electron) cooling timescale. This is reasonable and may be even conservative from the energetics requirement of neutrino-emitting AGN. For NGC 1068, the proton luminosity

would be  $10^{43} \text{ erg s}^{-1} \lesssim L_p \lesssim 10^{44} \text{ erg s}^{-1}$  [35,40], justifying  $C \sim 0.1\text{--}1$ . For TXS 0506 + 056, the proton luminosity in the single-zone model already violates the Eddington luminosity  $L_{\text{Edd}}$  [47], so our choice is conservative. This is also reasonable for electrons because of  $L_e \sim 8 \times 10^{47} \text{ erg s}^{-1} \sim 20L_{\text{Edd}}$  [79]. In principle, if the CR acceleration mechanism is understood, spectral modification due to BSM cooling may allow us to improve constraints and  $C \sim 1$  is possible. For proton energies of interest, we use 10–300 TeV for NGC 1068 [33], which is required to match the IceCube data [40]. For protons in TXS 0506 + 056, we use 0.1–20 PeV [43], and for electrons we use 50 GeV–2 TeV, following Ref. [79].

Applying the condition of Eq. (7) for NGC 1068 and TXS 0506 + 056, we set constraints on the DM-proton and DM-electron cross sections via a heavy mediator (see Fig. 3). The solid lines correspond to scenario I, and the dashed lines correspond to scenario II (see Table I). We find that our constraints become stronger at lower DM masses, due to the fact that the number density of DM particles increases, and the cross section needed to induce energy losses becomes smaller. However, for protons the dependence of the constraint on the DM mass is more pronounced than for electrons, since the elastic DM-proton cross section decreases with reference to its maximum value for  $E \gtrsim m_p^2/2m_{\text{DM}}$ .

For comparison, we show complementary constraints from other methods. The green region is excluded by DM direct detection experiments [88–94]. The cyan region is constrained by Milky Way satellite galaxy counts [95], and the gray region is constrained by big bang nucleosynthesis (constraints can be stronger by a factor as large as  $\sim 3$  depending on the details of the model) [96–99]. The orange region is constrained by CR-boosted DM at XENON1T [19], and the red regions are excluded when considering the blazar-boosted DM flux from TXS 0506 + 056 [22,52]. Finally, values above the brown line are constrained by CR-boosted DM at the Super-Kamiokande experiment [76]. Further, for DM-electron scatterings, we include constraints from the solar reflection [100], and the region of values where light thermal DM acquires its relic abundance via various mechanisms [12,87,101]. From Fig. 3, one sees that our constraints for light DM coupling to protons are stronger than complementary bounds for  $m_{\text{DM}} \lesssim 10^{-3} - 10^{-2} \text{ GeV}$ . Additional constraints from colliders may also apply; see, e.g., Ref. [102] for constraints on dark matter with masses above  $m_{\text{DM}} \gtrsim 0.1 \text{ GeV}$ , assuming a mediator of mass  $m_\phi \sim 1 \text{ GeV}$  and a direct coupling to quarks. If the mediator were more massive, or if it couples to gluons, those constraints could be weaker.

For DM-electron scatterings, our constraints are stronger than direct detection bounds at masses below  $m_{\text{DM}} \lesssim 5 \times 10^{-3} \text{ GeV}$ . In addition, for DM-electron interactions, AGN data allow one to probe the parameter space favored for DM models with  $m_{\text{DM}} \lesssim 10^{-4} \text{ GeV}$ . Effects of

different assumptions on the DM distribution and constraints in a concrete model of DM-proton interactions are discussed in Supplemental Material [103].

*Summary and discussion.* Recent multimessenger measurements of AGN have indicated that high-energy particles, in particular, CR protons and secondary neutrinos, are produced in the vicinity of SMBHs. CR cooling could be significantly enhanced by BSM interactions with DM, thanks to a large DM density around the central SMBH. We demonstrated that neutrino-emitting AGN, NGC 1068 and TXS 0506 + 056, allow us to set strong constraints on sub-GeV DM coupled to protons and/or electrons. The new constraints on light DM coupling to protons are stronger than other complementary bounds for  $m_{\text{DM}} \lesssim 10^{-3} - 10^{-2} \text{ GeV}$ . For DM-electron scatterings, our constraints are stronger than direct detection bounds at masses below  $m_{\text{DM}} \lesssim 5 \times 10^{-3} \text{ GeV}$ , which potentially allows us to probe the parameter space favored for thermal DM models with  $m_{\text{DM}} \lesssim 10^{-4} \text{ GeV}$ .

Remarkably, our method based on CR cooling is unique and different from previous AGN constraints from boosted DM [22] and those on neutrino-DM interactions [65,104–109], in that the results are largely insensitive to CR and neutrino spectra. Regarding uncertainties in CR cooling timescales, we stress that our constraints are robust and conservative for NGC 1068. This is because the neutrino production efficiency of CR protons has to be nearly maximal to explain the neutrino flux [40], and relaxing assumptions (e.g., with longer CR cooling timescales and/or softer CR spectra) will make the limits stronger. Future multimessenger observations and astrophysical modeling will allow us to better understand the sources and reduce uncertainties, and the resulting limits on the DM-proton and the DM-electron cross section will become more stringent and robust. Understanding acceleration mechanisms will also enable us to compare  $\tau_{\text{DM}-i}^{\text{el}}$  to the acceleration timescale for placing constraints.

Multimessenger observations of neutrino sources have been proposed to study DM interactions with photons [65] and neutrinos [65,104–111], as well as historically investigated annihilating or decaying signatures. Now there is accumulating evidence that AGN can accelerate CRs to TeV–PeV energies. We demonstrate that high-energy particle emission from AGN provides us with a powerful probe of DM scatterings with protons and electrons through CR interactions.

*Acknowledgments.* We are very grateful to Francesca Capel, Mar Císcar, Francesc Ferrer, Alejandro Ibarra, Walter Winter, Chengchao Yuan, and Bing Zhang for useful discussions. K. M. thanks the Topical Workshop: NGC 1068 as cosmic laboratory sponsored by (Sonderforschungsbereiche) SFB1258 and Cluster of Excellence

ORIGINS. G. H. is supported by the Collaborative Research Center SFB1258 and by the Deutsche Forschungsgemeinschaft (DFG, German Research Foundation) under Germany’s Excellence Strategy—EXC-2094–390783311.

K. M. is supported by the National Science Foundation Grants No. AST-1908689, No. AST-2108466, and No. AST-2108467 and KAKENHI No. 20H01901 and No. 20H05852.

- 
- [1] G. Bertone and D. Hooper, *Rev. Mod. Phys.* **90**, 045002 (2018).
- [2] G. Bertone, D. Hooper, and J. Silk, *Phys. Rep.* **405**, 279 (2005).
- [3] M. W. Goodman and E. Witten, *Phys. Rev. D* **31**, 3059 (1985).
- [4] R. Bernabei *et al.*, *Phys. Rev. D* **77**, 023506 (2008).
- [5] T. Marrodán Undagoitia and L. Rauch, *J. Phys. G* **43**, 013001 (2016).
- [6] R. Essig, J. Mardon, and T. Volansky, *Phys. Rev. D* **85**, 076007 (2012).
- [7] R. Essig, G. K. Giovanetti, N. Kurinsky, D. McKinsey, K. Ramanathan, K. Stifter, and T.-T. Yu, in *Proceedings of the 2022 Snowmass Summer Study* (2022), arXiv:2203.08297.
- [8] P. Hut, *Phys. Lett.* **69B**, 85 (1977).
- [9] B. W. Lee and S. Weinberg, *Phys. Rev. Lett.* **39**, 165 (1977).
- [10] C. Boehm and P. Fayet, *Nucl. Phys.* **B683**, 219 (2004).
- [11] L. J. Hall, K. Jedamzik, J. March-Russell, and S. M. West, *J. High Energy Phys.* 03 (2010) 080.
- [12] Y. Hochberg, E. Kuflik, T. Volansky, and J. G. Wacker, *Phys. Rev. Lett.* **113**, 171301 (2014).
- [13] A. N. Baushev, *Astrophys. J.* **771**, 117 (2013).
- [14] P. S. Behroozi, A. Loeb, and R. H. Wechsler, *J. Cosmol. Astropart. Phys.* **06** (2013) 019.
- [15] G. Besla, A. Peter, and N. Garavito-Camargo, *J. Cosmol. Astropart. Phys.* **11** (2019) 013.
- [16] G. Herrera and A. Ibarra, *Phys. Lett. B* **820**, 136551 (2021).
- [17] G. Herrera, A. Ibarra, and S. Shirai, *J. Cosmol. Astropart. Phys.* **04** (2023) 026.
- [18] A. Smith-Orlik *et al.*, *J. Cosmol. Astropart. Phys.* **10** (2023) 070.
- [19] T. Bringmann and M. Pospelov, *Phys. Rev. Lett.* **122**, 171801 (2019).
- [20] Y. Ema, F. Sala, and R. Sato, *Phys. Rev. Lett.* **122**, 181802 (2019).
- [21] J. Alvey, M. Campos, M. Fairbairn, and T. You, *Phys. Rev. Lett.* **123**, 261802 (2019).
- [22] J.-W. Wang, A. Granelli, and P. Ullio, *Phys. Rev. Lett.* **128**, 221104 (2022).
- [23] K. Agashe, Y. Cui, L. Necib, and J. Thaler, *J. Cosmol. Astropart. Phys.* **10** (2014) 062.
- [24] D. Kim, J.-C. Park, and S. Shin, *Phys. Rev. Lett.* **119**, 161801 (2017).
- [25] A. Das and M. Sen, *Phys. Rev. D* **104**, 075029 (2021).
- [26] C. V. Cappiello, N. P. A. Kozar, and A. C. Vincent, *Phys. Rev. D* **107**, 035003 (2023).
- [27] C. A. Argüelles, V. Muñoz, I. M. Shoemaker, and V. Takhistov, *Phys. Lett. B* **833**, 137363 (2022).
- [28] Y.-H. Lin, W.-H. Wu, M.-R. Wu, and H. T.-K. Wong, *Phys. Rev. Lett.* **130**, 111002 (2023).
- [29] T. N. Maity and R. Laha, *Eur. Phys. J. C* **84**, 117 (2024).
- [30] K. Murase, M. Ahlers, and B. C. Lacki, *Phys. Rev. D* **88**, 121301 (2013).
- [31] W. Winter, *Phys. Rev. D* **88**, 083007 (2013).
- [32] K. Murase, D. Guetta, and M. Ahlers, *Phys. Rev. Lett.* **116**, 071101 (2016).
- [33] R. Abbasi *et al.* (IceCube Collaboration), *Science* **378**, 538 (2022).
- [34] M. Ajello, K. Murase, and A. McDaniel, *Astrophys. J. Lett.* **954**, L49 (2023).
- [35] K. Murase, S. S. Kimura, and P. Meszaros, *Phys. Rev. Lett.* **125**, 011101 (2020).
- [36] A. Kheirandish, K. Murase, and S. S. Kimura, *Astrophys. J.* **922**, 45 (2021).
- [37] B. Eichmann, F. Oikonomou, S. Salvatore, R.-J. Dettmar, and J. Becker Tjus, *Astrophys. J.* **939**, 43 (2022).
- [38] Y. Inoue, D. Khangulyan, and A. Doi, *Astrophys. J. Lett.* **891**, L33 (2020).
- [39] S. Inoue, M. Cerruti, K. Murase, and R.-Y. Liu, *Proc. Sci. ICRC2023* (2023) 1161 [arXiv:2207.02097].
- [40] K. Murase, *Astrophys. J. Lett.* **941**, L17 (2022).
- [41] C. Blanco, D. Hooper, T. Linden, and E. Pinetti, arXiv: 2307.03259.
- [42] M. G. Aartsen *et al.* (IceCube, Fermi-LAT, MAGIC, AGILE, ASAS-SN, HAWC, H.E.S.S., INTEGRAL, Kanata, Kiso, Kapteyn, Liverpool Telescope, Subaru, Swift NuSTAR, VERITAS, VLA/17B-403 Collaborations), *Science* **361**, eaat1378 (2018).
- [43] M. G. Aartsen *et al.* (IceCube Collaboration), *Science* **361**, 147 (2018).
- [44] S. Ansoldi *et al.* (MAGIC Collaboration), *Astrophys. J. Lett.* **863**, L10 (2018).
- [45] A. Keivani *et al.*, *Astrophys. J.* **864**, 84 (2018).
- [46] P. Padovani, F. Oikonomou, M. Petropoulou, P. Giommi, and E. Resconi, *Mon. Not. R. Astron. Soc.* **484**, L104 (2019).
- [47] K. Murase, F. Oikonomou, and M. Petropoulou, *Astrophys. J.* **865**, 124 (2018).
- [48] S. Gao, A. Fedynitch, W. Winter, and M. Pohl, *Nat. Astron.* **3**, 88 (2019).
- [49] M. Cerruti, A. Zech, C. Boisson, G. Emery, S. Inoue, and J.-P. Lenain, *Mon. Not. R. Astron. Soc.* **483**, L12 (2018).
- [50] B. T. Zhang, M. Petropoulou, K. Murase, and F. Oikonomou, *Astrophys. J.* **889**, 118 (2020).
- [51] M. Petropoulou, K. Murase, M. Santander, S. Buson, A. Tohuvavohu, T. Kawamuro, G. Vasilopoulos, H.

- Negoro, Y. Ueda, M. H. Siegel, A. Keivani, N. Kawai, A. Mastichiadis, and S. Dimitrakoudis, *Astrophys. J.* **891**, 115 (2020).
- [52] A. Granelli, P. Ullio, and J.-W. Wang, *J. Cosmol. Astropart. Phys.* **07** (2022) 013.
- [53] S. Bhowmick, D. Ghosh, and D. Sachdeva, *J. Cosmol. Astropart. Phys.* **07** (2023) 039.
- [54] E. D. Bloom and J. D. Wells, *Phys. Rev. D* **57**, 1299 (1998).
- [55] M. Gorchtein, S. Profumo, and L. Ubaldi, *Phys. Rev. D* **82**, 083514 (2010).
- [56] D. Hooper and S. D. McDermott, *Phys. Rev. D* **97**, 115006 (2018).
- [57] C. V. Cappiello, K. C. Y. Ng, and J. F. Beacom, *Phys. Rev. D* **99**, 063004 (2019).
- [58] M. Cermeño, C. Degrande, and L. Mantani, *Phys. Rev. D* **105**, 083019 (2022).
- [59] A. Ambrosone, M. Chianese, D. F. G. Fiorillo, A. Marinelli, and G. Miele, *Phys. Rev. Lett.* **131**, 111003 (2023).
- [60] P. J. E. Peebles, *Gen. Relativ. Gravit.* **3**, 63 (1972).
- [61] G. D. Quinlan, L. Hernquist, and S. Sigurdsson, *Astrophys. J.* **440**, 554 (1995).
- [62] P. Gondolo and J. Silk, *Phys. Rev. Lett.* **83**, 1719 (1999).
- [63] P. Ullio, H. Zhao, and M. Kamionkowski, *Phys. Rev. D* **64**, 043504 (2001).
- [64] F. Ferrer, A. M. da Rosa, and C. M. Will, *Phys. Rev. D* **96**, 083014 (2017).
- [65] F. Ferrer, G. Herrera, and A. Ibarra, *J. Cosmol. Astropart. Phys.* **05** (2023) 057.
- [66] J. F. Navarro, C. S. Frenk, and S. D. M. White, *Astrophys. J.* **490**, 493 (1997).
- [67] J. F. Navarro, C. S. Frenk, and S. D. M. White, *Astrophys. J.* **462**, 563 (1996).
- [68] T. Lacroix, M. Karami, A. E. Broderick, J. Silk, and C. Böhm, *Phys. Rev. D* **96**, 063008 (2017).
- [69] T. Di Matteo, R. A. C. Croft, V. Springel, and L. Hernquist, *Astrophys. J.* **593**, 56 (2003).
- [70] L. Ferrarese, *Astrophys. J.* **578**, 90 (2002).
- [71] O. Piana, P. Dayal, M. Volonteri, and T. R. Choudhury, *Mon. Not. R. Astron. Soc.* **500**, 2146 (2020).
- [72] T. Lacroix, C. Böhm, and J. Silk, *Phys. Rev. D* **92**, 043510 (2015).
- [73] T. Lin, H.-B. Yu, and K. M. Zurek, *Phys. Rev. D* **85**, 063503 (2012).
- [74] R. Essig, E. Kuflik, S. D. McDermott, T. Volansky, and K. M. Zurek, *J. High Energy Phys.* **11** (2013) 193.
- [75] M. Cirelli, N. Fornengo, B. J. Kavanagh, and E. Pinetti, *Phys. Rev. D* **103**, 063022 (2021).
- [76] K. Abe *et al.* (Super-Kamiokande Collaboration), *Phys. Rev. Lett.* **130**, 031802 (2023).
- [77] K. Bondarenko, A. Boyarsky, T. Bringmann, M. Hufnagel, K. Schmidt-Hoberg, and A. Sokolenko, *J. High Energy Phys.* **03** (2020) 118.
- [78] I. Angeli, *At. Data Nucl. Data Tables* **87**, 185 (2004).
- [79] A. Keivani, K. Murase, M. Petropoulou, D. B. Fox, S. B. Cenko, S. Chaty, A. Coleiro, J. J. DeLaunay, S. Dimitrakoudis, P. A. Evans, J. A. Kennea, F. E. Marshall, A. Mastichiadis, J. P. Osborne, M. Santander, A. Tohuvavohu, and C. F. Turley, *Astrophys. J.* **864**, 84 (2018).
- [80] G. Elor, R. McGehee, and A. Pierce, *Phys. Rev. Lett.* **130**, 031803 (2023).
- [81] P. N. Bhattacharjee, G. Elor, R. McGehee, and A. Pierce, *J. High Energy Phys.* **01** (2023) 128.
- [82] J. Smirnov and J. F. Beacom, *Phys. Rev. Lett.* **125**, 131301 (2020).
- [83] A. Parikh, J. Smirnov, W. L. Xu, and B. Zhou, *J. High Energy Phys.* **08** (2023) 091.
- [84] R. Essig *et al.*, *arXiv:2203.08297*.
- [85] R. Essig, M. Fernandez-Serra, J. Mardon, A. Soto, T. Volansky, and T.-T. Yu, *J. High Energy Phys.* **05** (2016) 046.
- [86] Y. Hochberg, E. Kuflik, H. Murayama, T. Volansky, and J. G. Wacker, *Phys. Rev. Lett.* **115**, 021301 (2015).
- [87] E. Kuflik, M. Perelstein, N. R.-L. Lorier, and Y.-D. Tsai, *Phys. Rev. Lett.* **116**, 221302 (2016).
- [88] A. H. Abdelhameed *et al.* (CRESST Collaboration), *Phys. Rev. D* **100**, 102002 (2019).
- [89] C. Amole *et al.* (PICO Collaboration), *Phys. Rev. D* **93**, 052014 (2016).
- [90] L. Barak *et al.*, *Phys. Rev. Lett.* **125**, 171802 (2020).
- [91] E. Aprile *et al.*, *Phys. Rev. Lett.* **123**, 251801 (2019).
- [92] T. Emken, C. Kouvaris, and I. M. Shoemaker, *Phys. Rev. D* **96**, 015018 (2017).
- [93] T. Emken, R. Essig, C. Kouvaris, and M. Sholapurkar, *J. Cosmol. Astropart. Phys.* **09** (2019) 070.
- [94] M. S. Mahdawi and G. R. Farrar, *J. Cosmol. Astropart. Phys.* **10** (2018) 007.
- [95] M. A. Buen-Abad, R. Essig, D. McKeen, and Y.-M. Zhong, *Phys. Rep.* **961**, 1 (2022).
- [96] N. Sabti, J. Alvey, M. Escudero, M. Fairbairn, and D. Blas, *J. Cosmol. Astropart. Phys.* **01** (2020) 004.
- [97] G. Krnjaic and S. D. McDermott, *Phys. Rev. D* **101**, 123022 (2020).
- [98] P. F. Depta, M. Hufnagel, K. Schmidt-Hoberg, and S. Wild, *J. Cosmol. Astropart. Phys.* **04** (2019) 029.
- [99] C. Giovanetti, M. Lisanti, H. Liu, and J. T. Ruderman, *Phys. Rev. Lett.* **129**, 021302 (2022).
- [100] H. An, M. Pospelov, J. Pradler, and A. Ritz, *Phys. Rev. Lett.* **120**, 141801 (2018).
- [101] R. Essig, T. Volansky, and T.-T. Yu, *Phys. Rev. D* **96**, 043017 (2017).
- [102] N. Daci, I. De Bruyn, S. Lowette, M. H. G. Tytgat, and B. Zaldívar, *J. High Energy Phys.* **11** (2015) 108.
- [103] See Supplemental Material at <http://link.aps.org/supplemental/10.1103/PhysRevD.110.L011701> for a discussion on the dependence of our constraints on the distribution of dark matter particles in the AGN, the conditions for adiabatic growth in NGC 1068 and TXS 0506+056, and for a comparison of our bounds in a concrete model of dark matter-nucleon interactions with complementary bounds on new scalar mediators.
- [104] K. J. Kelly and P. A. N. Machado, *J. Cosmol. Astropart. Phys.* **10** (2018) 048.
- [105] K.-Y. Choi, J. Kim, and C. Rott, *Phys. Rev. D* **99**, 083018 (2019).
- [106] K. Murase and I. M. Shoemaker, *Phys. Rev. Lett.* **123**, 241102 (2019).
- [107] J. Alvey and M. Fairbairn, *J. Cosmol. Astropart. Phys.* **07** (2019) 041.

- [108] J. M. Cline, S. Gao, F. Guo, Z. Lin, S. Liu, M. Puel, P. Todd, and T. Xiao, [Phys. Rev. Lett.](#) **130**, 091402 (2023).
- [109] J. M. Cline and M. Puel, [J. Cosmol. Astropart. Phys.](#) **06** (2023) 004.
- [110] C. A. Argüelles, A. Kheirandish, and A. C. Vincent, [Phys. Rev. Lett.](#) **119**, 201801 (2017).
- [111] R. Eskenasy, A. Kheirandish, and K. Murase, [Phys. Rev. D](#) **107**, 103038 (2023).